JOURNAL OF MATERIALS SCIENCE 22 (1987) 3901–3906

Creep-fatigue interaction in eutectic lead–tin solder alloy

R. C. WEINBEL, J. K. TIEN
Centre for Strategic Materials, Henry Krumb School of Mines, Columbia University, New York, USA

R. A. POLLAK, S. K. KANG
IBM, T. J. Watson Research Centre, Yorktown Heights, New York, USA

A test protocol pivoting about stress cycling where the load waves were trapazoidal and the cycling frequency controlled by balanced time on load and off load was used to determine frequency, mean tensile stress, and compressive stress effects on the creep-fatigue behaviour of the Pb–Sn eutectic solder alloy at ambient temperature. It is consistently found that the minimum creep (or cyclic creep) rate decreases as frequency increases, that is, as hold time decreases. Both the number of cycles to failure as well as the time to failure increases as frequency increases. The cyclic creep rate increases drastically and the number of cycles to failure decreases drastically as the mean applied stress is increased. These results are consistent with anelastic strain recovery mechanism for creep–fatigue interaction. Similar results are also found in butt-joint solder junction configured specimens.

1. Introduction

Many investigations have been conducted on the creep properties of the Pb–Sn eutectic alloys [1–7]. Even at ambient temperatures these alloys are at 0.65 of the absolute melting temperature. In addition to high homologous temperature, these solder alloys are often subjected to a cyclic loading condition imposed by thermal stresses. These conditions have been studied for solder joints and bulk specimens under the conditions of power cycling [8, 9], thermal cycling [10], and stress/strain cycling [11].

Pb–Sn alloys are now used extensively not only as conventional solder junctions, but also as junctions in micro-electronic chip assemblies. Recently, the electronics and computer industry has shown interest in surface mount technology – a scheme wherein the typical "plated through hole" filled with solder and chip lead, is replaced with a pad on the substrate surface and a simple solder joint joining this pad to the chip lead. Fig. 1 shows examples of both packaging schemes. While surface mount technology provides the advantages of lower production costs and increased board density, it places the full load-bearing responsibility on the solder joint itself. Stresses induced in these joints can be high and cyclic. Although some studies have been conducted in an effort to reduce the failure of these joints, most have attempted to classify the various solder alloys on the basis of simple mechanical properties such as tensile or shear strength, creep resistance, or thermal resistance [1–4]. As some researchers have pointed out however [5, 10], these rankings may vary from test to test, from bulk to joint configuration, and alloy purity.

We believe that the pertinent mechanical behaviour of Pb–Sn solders can be best understood through creep–fatigue interaction studies. Creep–fatigue interaction typically describes the cyclic application of a load at temperatures where time dependent, thermally activated processes can occur. Creep–fatigue testing can be broken down into the following protocols [9].

1. Conventional low cycle fatigue tests at high homologous temperatures
2. Tests involving the intermittent application of creep and fatigue loading
3. Low cycle fatigue tests at elevated temperatures involving variable hold times (variable frequencies) and mean stresses.

For this investigation, the type (3) protocol was followed, since the resulting information is more conducive to unique interpretation and because the hold time aspects do mimic actual practice involving the solder joints. As mentioned, the goal of this type of testing is first to enable the systematic definition of effects, and then to understand the physical processes that are occurring. With these results it is hoped that, (i) the long-term service life of a component may be predicted from short-term laboratory tests, and (ii) the inputs will be valuable for the alloy and microstructural design of more reliable solder systems.

2. Experimental procedure

The eutectic Pb–Sn alloy used in this study is a commercial grade solder alloy of nominal composition in weight percent of 63Sn–37Pb. A compositional analysis for the alloy is shown in Table I. The alloy was supplied in rectangular bar form which was then remelted and cast into a 1.59 cm diameter cylindrical mold at room temperature. The cylindrical ingot was then machined to the finished button-head specimen

0022–2461/87 $03.00 + .12

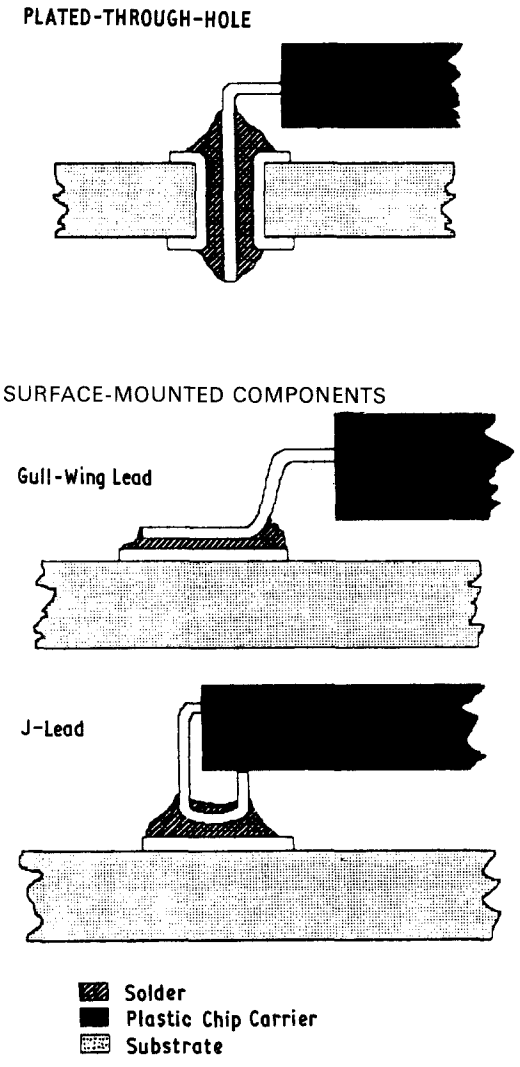

Figure 1 Schematic drawings of a typical plated-through-hole solder joint, and two common surface mounted joints.

with 2.54 cm gauge length and 0.635 cm gauge diameter. This casting procedure produced a two phase eutectic structure with 32 vol % of the Pb-rich solid solution and with mean inter-lamellar spacings varying from 1.5. to 4.9 μm. Fig. 2 shows the typical eutectic microstructure found in the specimen gauge length. This microstructure is very similar to that found in actual package joints, which typically have a lamellar spacing of approximately 1.5 μm [12].

Quantitative metallography of the eutectic alloy proved to be difficult due to the soft nature of both phases, but quite necessary due to the anticipated sensitivity of mechanical properties to microstructure [12, 13]. We found that the best results for microstructural characterization were attained by grinding the specimen from 240 to 600 grit, etching the surface in concentrated HCl for 5 sec, then carefully grinding on 600 grit paper again. We then chose to electropolish, at 25° C, with a 10% Perchloric-Ethanol solution, at 12–15 volts for 5–15 sec. The specimens were then characterized using a JSM 35cf SEM in SEI mode.

Specimens were chosen at random from the eutectic

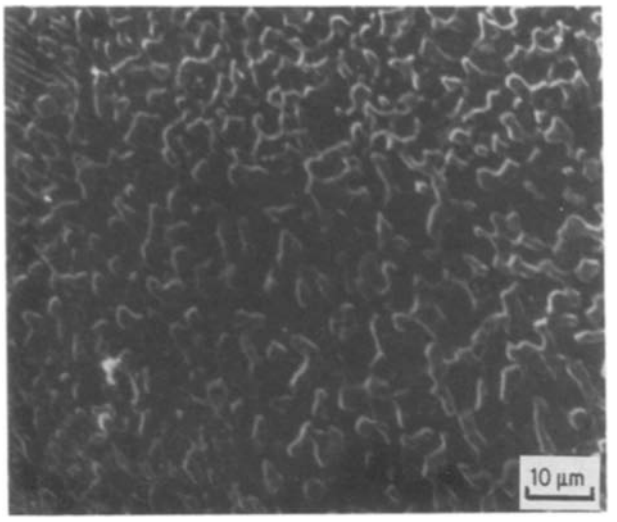

Figure 2 Micrograph of typical Pb–Sn eutectic alloy. The specimen was electropolished, and then photographed in SEM in SEI mode (light colour is Pb-rich phase).

series, sections were taken from the gauge length (transverse and longitudinal) and button-head section to evaluate the consistency of the microstructure. Each SEM metallography specimen was observed at four locations (typically at 2000 ×), where it was photographed for later measurements to determine lamellar spacing. After mechanical testing, the fracture surface of each specimen was cut from the remaining gauge length, for SEM fracture analysis. At the same time, an SEM metallography sample was cut from the gauge length and the button-head of the same specimen.

Although the main focus of the study was on the creep–fatigue interaction in these Pb–Sn alloys, tensile tests were performed on each alloy at various strain rates. These were necessary in order to insure that the maximum stress attained in the cyclic creep tests was below the yield stress. In addition, we sought to provide a reliable data base of eutectic alloy data, since as mentioned in the introduction, the literature values are sometimes inconsistent or poorly documented.

All of the cyclic creep experiments were performed on a computer controlled servo-hydraulic MTS testing machine at 25° C ± 2° C. Two sets of cyclic creep tests were performed using the eutectic alloy, one with load cycling between 0.138 and 13.8 MPa, the other between 0.138 and 27.6 MPa. These were essentially $R = 0$ tests where the maximum or mean stress was the variable and where both maximum stresses were below the yield stress of the eutectic alloy at 25° C. In addition, the other important variable for each set of these cyclic creep tests was hold time or frequency. The load was cycled such that the time at maximum load equalled the time at minimum load and the hold times were 4 times as long as the ramp times. The testing frequencies were 100 cycles per minute (cpm),

TABLE I Evaluated eutectic alloy composition (all values in weight percent)

Alloy	Sn	Pb	Cu	Bi	In	Sb	Ag	Al
Eutectic	63.1	Bal.	0.0001	0.0002	0.0001	–	0.0001	–

10 cpm, and 0.1 cpm. These testing conditions are equivalent to load controlled low cycle fatigue, where trapazoidal wave loading is employed, with an R value of approximately 0.01. The non-zero minimum load was necessary in order to maintain load train tension at all times.

Four additional cyclic tests were performed at a hold time of 3 sec in order to further discern the influence of mean stress on life. One test had a minimum stress of 0.138 MPa and a maximum stress of 20.7 MPa. Another cycled between 13.8 and 27.6 MPa. Two tension-compression tests were performed: one cycled between −11.8 and 14.5 MPa, the other between −29.0 and 25.5 MPa.

The strain was measured using an extensometer and LVDT connected to the MTS computer via an A/D converter. The strain measuring system is capable of resolving strains of 5×10^{-5}. Both stress and strain were monitored 256 times each cycle and for specified cycles this data was recorded on disk. Later this data was downloaded from the MTS digital PDP-11 computer to an IBM PC where it was analysed to determine life, in terms of cycles and/or time, envelope strain, and minimum net strain rate.

In addition to the cyclic creep testing, static creep stress rupture tests were performed at 25° C on a deadload creep machine. Stresses of 6.9, 13.8 and 27.6 MPa were used to investigate the effect of stress on the minimum creep rate of the eutectic Sn–Pb alloy.

Finally, joint specimens of the eutectic alloy were constructed and mechanically tested to observe the effects of load cycling frequency on the cycles or time to failure. The joint was of the butt-joint configuration and consisted of copper ends in the shape of one half of a button-head test specimen, and eutectic solder reflowed into the joint between the two copper halves. A steel jig was constructed to help align the specimen, and to control joint thickness during joint formation. After fluxing the copper bases with a zinc-chloride flux, they were placed in the jig and heated to approximately 220° C. A eutectic Pb–Sn preform was then placed between the copper halves, and upon reflowing, the copper halves were allowed to set to the predetermined joint thickness of approximately 250 μm. The whole assembly was subsequently cooled with moving air to 180° C, and then quenched in water to room temperature. Each specimen then received a 600 grit finish, and joint thicknesses were measured at approximately 350 × on a Zeiss optical microscope. Cyclic creep testing was conducted at 25° C on the MTS testing machine. The cyclic creep tests were performed at a minimum stress of 0.138 MPa, and a maximum stress of 55.2 MPa, at frequencies of 0.1 and 100 cpm. One cyclic creep test was performed at a maximum stress of 27.6 MPa, but because no detectable creep rate was measured after 60 h on load, the test was stopped and all following tests on the joint specimens were conducted at a maximum stress of 55.2 MPa. These higher stress values were used because the yield stress of the joint configuration is 2 to 4 times higher than bulk values [14, 15].

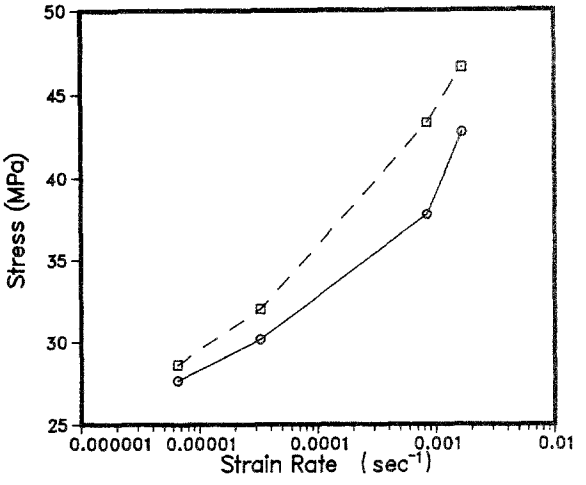

Figure 3 Results of tensile testing of the Pb–Sn eutectic at 25° C as a function of strain rate. (○) Yield stress, (□) ultimate tensile stress.

3. Results and discussion

3.1. Static results

Static creep testing, and tensile testing were performed on the eutectic alloy at 25° C. Yield stress and ultimate tensile stress are plotted as a function of strain rate, in Fig. 3. As previous authors have noted [13, 16, 17], the eutectic alloy exhibits rate sensitive deformation, indicative of thermally-assisted plastic flow.

The creep results are plotted in Fig. 4, as natural log of steady state creep rate as a function of natural log applied stress. This plot revealed the exponent n, in the steady-state creep equation

$$\varepsilon_{ss} = A(\sigma/E)^n \exp[-Q/RT] \quad (1)$$

where ε_{ss} is the steady state or minimum creep rate, A is a structure dependent constant, σ is the applied stress, E is the Young's modulus, n is the apparent stress exponent, Q is the activation energy, and RT have their usual meaning. From the plot, n was determined to be 5.6, with a correlation coefficient of 0.995. This falls within the range of 4 to 10 noted in earlier works [4, 18].

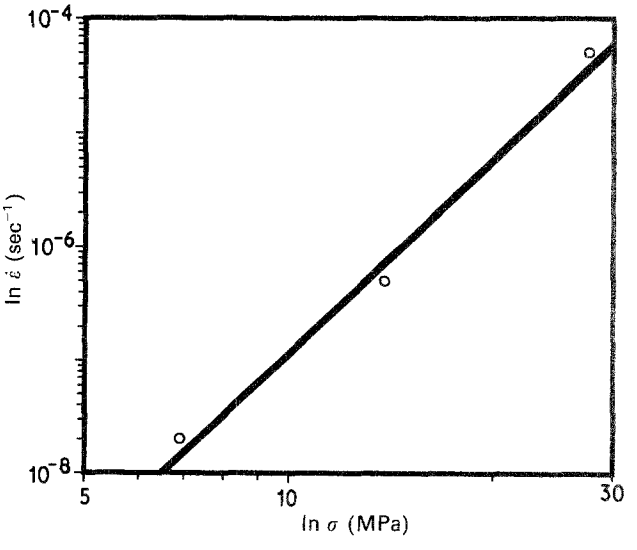

Figure 4 Static creep results for Pb–Sn eutectic at 25° C, tested at 6.9, 13.8, and 27.6 MPa. The slope reveals the steady-state creep exponent, n, to have a value of 5.6.

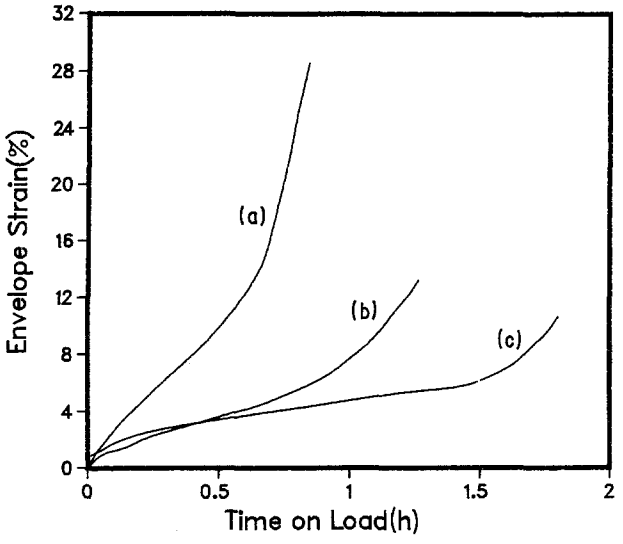

Figure 5 Envelope strain curves are drawn for a static and two cyclic creep curves. The hold time during load cycling are (a) static, (b) 300 sec, (c) 0.3 sec. All of these tests were performed at 25° C, with a maximum load of 27.6 MPa. A third cyclic creep curve (hold time of 3 sec) has been omitted for clarity.

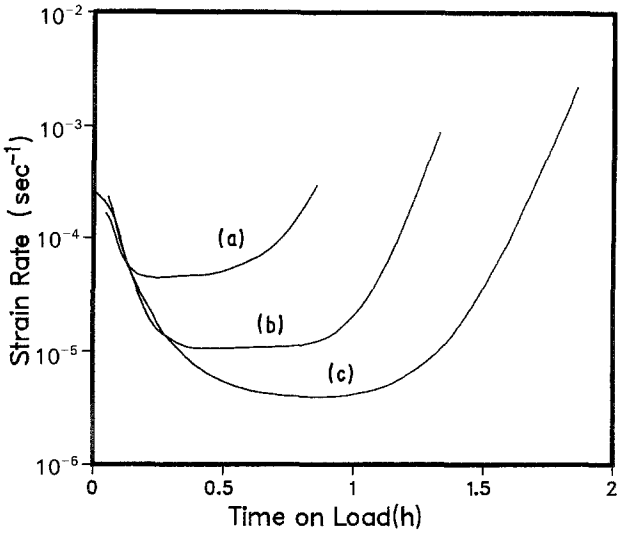

Figure 6 This is a differential plot of the envelope strain curves in Fig. 4. Strain rate is plotted against time on load, for the eutectic alloy tested at 25°C and maximum stress 27.6 MPa. One curve has been omitted for clarity. Hold times are (a) static, (b) 300 sec, (c) 0.3 sec.

3.2. Frequency effect

Cyclic creep curves were generated for each cyclic test in the following manner, as described by Nardone *et al.* [19]. First, a smooth curve is drawn through the points of maximum strain for each on-load cycle, to generate an envelope strain curve. The initial point of the envelope strain curve is taken from the first cycle as soon as the load reaches its maximum value. In this way, the elastic strain is not included in the envelope strain. The envelope strain is then plotted against the time on load to generate a cyclic creep curve. From this curve the rupture life (total time on load) and minimum creep rate can be determined for direct comparison to the same parameters of the static creep test.

A static and two cyclic creep curves are shown in Figs 5 and 6, for tests conducted at a maximum stress of 27.6 MPa. The times shown for each of the curves correspond to the time on load per cycle (defined as one-half the cyclic period). The static test was performed at the same maximum load as was used in the cyclic tests. From these figures it can be seen that the minimum strain rate decreases, while the cycles to failure increases with increasing cyclic frequency, or decreasing hold time. The lives to failure also increase, although not so dramatically.

Similar trends were observed for the eutectic alloy cyclically loaded at a maximum stress of 13.8 MPa. Consistently, there is a decrease in the minimum creep rate by a factor of 6 to 8 when comparing a static test to a cyclic test with a frequency of 100 cpm at both maximum stresses. This frequency dependence of the minimum strain rate is shown graphically in Fig. 7, for cyclic creep tests at a maximum stress of 13.8 MPa, and a maximum stress of 27.6 MPa.

This dependence of minimum creep rate, and cycles and/or time to failure on cycling frequency has been observed previously for two particle strengthened alloys [19, 20]. The effect of frequency on the rupture life and minimum strain rate can be attributed to the storage and recovery of anelastic strain. When the storage of anelastic strain acts to delay nonrecoverable creep, a decrease in the cyclic creep rate will result from increasing the cycling frequency. The frequency dependence of the cyclic minimum strain rate is a function of the ratio of anelastic strain storage to nonrecoverable creep. The greater the frequency, the greater is the ratio of anelastic strain storage to nonrecoverable creep during the on-load cycles. The anelastic strain does not contribute to the net cyclic creep rate because it is recovered during the following off-load period, and as is observed, the greater the frequency the greater the decrease in net cyclic strain rate. This observation, and the fact that both cycles to failure and lives to failure are affected by frequency (or time on load), indicates that the creep–fatigue interaction in the Pb–Sn eutectic is more than just creep controlling the interaction. With creep control, cycles to failure is affected whereas lives or times to failure are constant and depend only on total time on load.

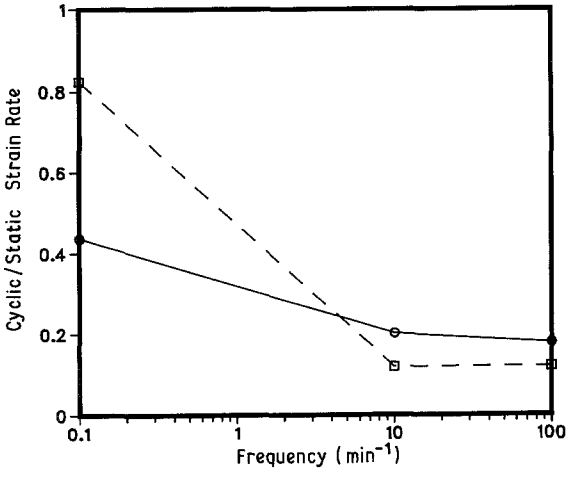

Figure 7 The ratio of cyclic strain rate to static strain rate is plotted against cyclic frequency for the eutectic alloy Pb–Sn eutectic at 25° C tested at two different maximum stresses. (——) Maximum stress 27.6 MPa, (– – –) maximum stress 13.8 MPa.

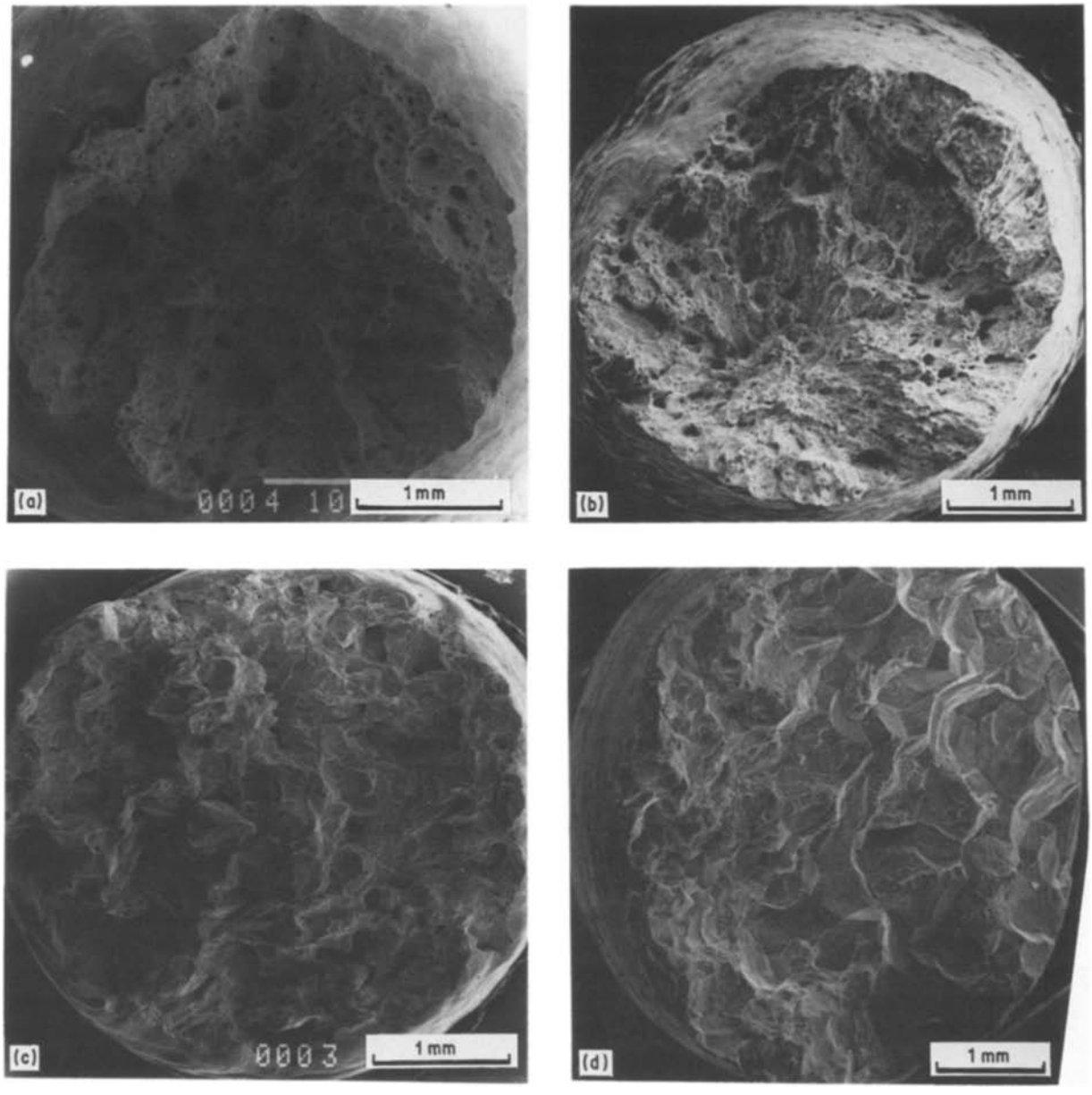

Figure 8 SEM micrographs of fracture surfaces of Pb–Sn eutectic specimens tested at a maximum stress of 27.6 MPa. The hold times are (a) static, (b) 300 sec, (c) 3 sec, (d) 0.3 sec.

The fracture surfaces for specimens from the series tested at a maximum stress of 27.6 MPa are shown in Fig. 8. It is interesting to note that as the frequency of load cycling is decreased from 100 cpm to statically loaded, the fracture surfaces shows an increase in the number and size of voids. The implication is that void formation, which is a prelude to creep rupture at high homologous temperatures, is aggravated by static loading in the eutectic Pb–Sn alloy.

In order to ensure that the same frequency effect was present in solder joints, joint specimens (joint thickness was approximately 250 μm) were tested as mentioned in the procedure, at a maximum stress of 55.2 MPa. The lifetime results for the static and two cyclic creep tests are plotted as a function of cyclic frequency in Fig. 9. The joint configuration, like the bulk alloy, showed an increase in lifetime as cyclic frequency increases.

3.3. Mean stress effect

The effect of mean stress on the cyclic creep behaviour of Pb–Sn eutectic was also considered for the cycling

TABLE II Mean stress data for cyclic creep in Pb–Sn eutectic (all tests conducted at a frequency of 10 cpm)

Mean stress (MPa)	Stress range (MPa)	No. cycles to failure	Total time on load (h)
6.9	13.8	Test stopped @ 100, 000 cycles (84 h)	
20.8	13.8	520	0.43
10.4	20.6	10 824	9.02
1.3	26.3	Test stopped @ 25, 000 cycles (20.8 h)	
13.9	27.5	1 516	1.27
−1.7	54.5	2 500	2.08

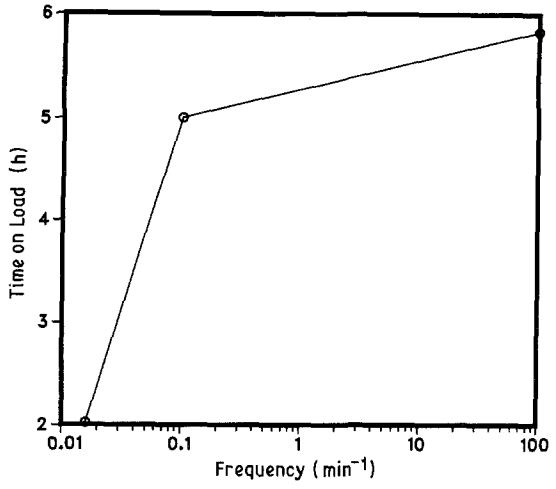

Figure 9 Lifetime results of cyclic creep testing for Pb–Sn eutectic joint specimens tested at a maximum stress of 55.2 MPa. (The static test was given a frequency of 1/2 of the rupture life.)

frequency of 10 cpm. The results of these tests are listed in Table II. The lifetime increases by over 2 orders of magnitude with a decrease in mean stress from 20.7 to 6.9 MPa for the stress range of 13.8 MPa. At least an order of magnitude increase in life was provided by decreasing the mean stress from 13.8 to 0.0 MPa at the stress range of 27.6 MPa. A similar effect is also observed in this data if only the tensile portion of the stress cycle is considered. Considering either interpretation, this sharp dependence of cyclic creep behaviour on mean stress is consistent with creep component being generally detrimental and with the anelastic model for cyclic creep [20]. More work is necessary to separate the importance of the compressive component of the stress cycle.

4. Concluding remarks

The results of this creep–fatigue investigation can have some direct practical consequences in the application of Pb–Sn solders and components. Consider for instance the increase in life as the frequency of cycling is increased. Intuitively, one may think that as a solder joint is cycled, it will fail upon reaching a certain number of cycles, and hence the higher the frequency of cycling, or shorter the hold time on load, the shorter the lifetime. In fact, as noted earlier, both an increase in cycles to failure and time on load to failure were seen for higher load cycling frequencies. Consequently, there may be no penalty for increased power on and off cycles in intermittent consumer electronic and computer applications. On the negative side, any form of accelerated testing, must consider the frequency effects in its evaluation of bulk Pb–Sn solder or components.

The extremely sharp dependence of cyclic life on mean stress underscores the sensitivity of solder joint reliability to design stresses at these high homologous temperatures where nonrecoverable creep is exponentially dependent on applied stress.

The investigation continues in order to define other effects and to enable the quantitative understanding of creep fatigue interactions in the Pb–Sn alloys. The effects of temperature, unbalanced cycles, plastic strain increments (cycling above yield stress), and alloy composition and microstructure are being determined [21]. As reported in the previous section, the effects of butt-joint junction thickness on strength and creep fatigue resistance are also being determined [15]. The results so far indicate that an anelastic strain recovery mechanism dominates the creep–fatigue interaction of the Pb–Sn eutectic alloy. This mechanism is sensitive to the strong dislocation pinning points such as the interparticle spacing between the Pb-rich phases in the alloy. It is interesting to note that preliminary results from a 81Pb–19Sn alloy (with the same solidus temperature as the eutectic alloy) show that its creep fatigue resistance is much less than that of the eutectic alloy as a consequence of much larger interparticle spacings [22].

Acknowledgements

We thank the IBM T. J. Watson Research Laboratories, and V. G. Veeraraghavan and A. K. Trivedi of IBM Endicott Laboratories for sponsoring this research. We acknowledge Mr. Erik Schwarzkopf and Dr. Thomas Caulfield for their helpful discussions.

References

1. D. O. ROSS, in Proceedings of 4th annual International Electronics Packaging Conference, Baltimore, October 1984, pp. 181–187.
2. R. HORIUCHI, A. B. EL-SEBAI and M. OTSUKA, *Phys. Stat. Sol.* **21** (1974) K89.
3. R. N. WILD, "Properties of Some Low Melt Fusible Solder Alloys", presented at INTERNEPCON, Brighton, England, October 1971.
4. D. GRIVAS, K. L. MURTY and J. W. MORRIS, Jr., *Acta Metall.* **28** (1979) 731.
5. F. A. MOHAMED and T. G. LANDGON, *Acta Met.* **23** (1975) 697.
6. J. H. SCHNEIBEL and P. M. HAZZLEDINE, *Scripta Metall.* **11** (1977) 953.
7. W. A. BAKER, *J. Inst. of Metals* **65** (1939) 277.
8. W. ENGELMAIER, in Proceedings of 4th annual International Electronics Packaging Conference, Baltimore, October 1984, pp. 539–546.
9. W. ENGELMAIER, *Circuit World* **11**, no. 3 (1985) 61.
10. R. N. WILD, *Welding Research Supplement,* November 1972, pp. 521s–526s.
11. R. N. WILD, "Some Fatigue Properties of Solders and Solder Joints", presented at INTERNEPCON, Brighton, England, October, 1975.
12. H. J. RACK and J. K. MAURIN, *J. Test. & Ev.*, **2** no. 5 (1974) 351.
13. B. P. KASHYAP and G. S. MURTY, *Mater. Sci. & Eng.* **50** (1981) 205.
14. H. H. MANKO, "Solders and Soldering", 2nd edn., (McGraw-Hill, New York, 1979).
15. R. C. WEINBEL, J. STEFANI and J. K. TIEN, unpublished research (1986).
16. H. E. CLINE and T. H. ALDEN, *Met. Trans.* **239** (1967) 710.
17. M. CAGNON, M. SUERY, A. EBERHARDT and B. BAUDELET, *Acta Met.* **25** (1977) 71.
18. G. S. MURTY, *J. Mat. Sci.* **8** (1973) 611.
19. V. C. NARDONE, D. E. MATEJCZYK and J. K. TIEN, *Met. Trans. A* **14A** (1983) 1435.
20. V. C. NARDONE and J. K. TIEN, *Met. Trans. A* **17A** (1986) 1577.
21. B. C. HENDRIX and J. K. TIEN, unpublished research.
22. R. C. WEINBEL, E. A. SCHWARZKOPF and J. K. TIEN, *Scripta Met.*, in press.

Received 6 November 1986
and accepted 28 January 1987